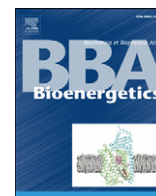Contents lists available at ScienceDirect

Biochimica et Biophysica Acta

journal homepage: www.elsevier.com/locate/bbabio

BBA
Bioenergetics

Femtosecond primary charge separation in *Synechocystis* sp. PCC 6803 photosystem I

Ivan V. Shelaev [a,c], Fedor E. Gostev [a], Mahir D. Mamedov [b], Oleg M. Sarkisov [a], Victor A. Nadtochenko [a,c,*], Vladimir A. Shuvalov [b,*], Alexey Yu. Semenov [b,*]

[a] N.N. Semenov Institute of Chemical Physics, Russian Academy of Sciences, Moscow, Russia
[b] A.N. Belozersky Institute of Physical–Chemical Biology, Moscow State University, Moscow, Russia
[c] Moscow Institute of Physics and Technology, Dolgoprudny, Russia

ARTICLE INFO

ABSTRACT

The ultrafast (<100 fs) conversion of delocalized exciton into charge-separated state between the primary donor P700 (bleaching at 705 nm) and the primary acceptor A_0 (bleaching at 690 nm) in photosystem I (PS I) complexes from *Synechocystis* sp. PCC 6803 was observed. The data were obtained by application of pump–probe technique with 20-fs low-energy pump pulses centered at 720 nm. The earliest absorbance changes (close to zero delay) with a bleaching at 690 nm are similar to the product of the absorption spectrum of PS I complex and the laser pulse spectrum, which represents the efficiency spectrum of the light absorption by PS I upon femtosecond excitation centered at 720 nm. During the first ~60 fs the energy transfer from the chlorophyll (*Chl*) species bleaching at 690 nm to the *Chl* bleaching at 705 nm occurs, resulting in almost equal bleaching of the two forms with the formation of delocalized exciton between 690-nm and 705-nm *Chl*s. Within the next ~40 fs the formation of a new broad band centered at ~660 nm (attributed to the appearance of *Chl* anion radical) is observed. This band decays with time constant simultaneously with an electron transfer to A_1 (phylloquinone). The subtraction of kinetic difference absorption spectra of the closed (state $P700^+A_0A_1$) PS I reaction center (RC) from that of the open (state $P700A_0A_1$) RC reveals the pure spectrum of the $P700^+A_0^-$ ion–radical pair. The experimental data were analyzed using a simple kinetic scheme: $An^* \xrightarrow{k1} [(PA_0)^*A_1 \xrightarrow{<100\,fs} P^+A_0^-A_1] \xrightarrow{k2} P^+A_0A_1^-$, and a global fitting procedure based on the singular value decomposition analysis. The calculated kinetics of transitions between intermediate states and their spectra were similar to the kinetics recorded at 694 and 705 nm and the experimental spectra obtained by subtraction of the spectra of closed RCs from the spectra of open RCs. As a result, we found that the main events in RCs of PS I under our experimental conditions include very fast (<100 fs) charge separation with the formation of the $P700^+A_0^-A_1$ state in approximately one half of the RCs, the ~5-ps energy transfer from antenna *Chl** to $P700A_0A_1$ in the remaining RCs, and ~25-ps formation of the secondary radical pair $P700^+A_0A_1^-$.

1. Introduction

The three-dimensional structure of photosystem (PS) I from the thermophilic cyanobacterium *Synechococcus elongatus* resolved using X-ray diffraction to resolution 2.5 Å has been reported [1]. The core of the complex consists of two large subunits (products of expression of genes *PsaA* and *PsaB*), which bind to 96 molecules of chlorophyll (*Chl*) *a*, 22 molecules of β-carotene, two molecules of phylloquinone, and an interpolypeptide iron–sulfur center F_X. Most *Chl a* molecules serve as antenna pigments. The primary electron donor P700 comprises two molecules of *Chl* (designated by us [2] as *ChlA1/ChlB1*), the porphyrin planes of the molecules being parallel to one another (distance, 3.6 Å) and perpendicular to the membrane plane. The X-ray diffraction analysis of crystals of the PS I complexes also (in addition to P700) revealed two domains of high electron density, which were attributed to *Chl a* molecules (*ChlA2/ChlB2*), in positions corresponding to accessory bacteriochlorophyll molecules in reaction center (RC) of purple bacteria, two *Chl a* molecules (*ChlA3* and *ChlB3*) in positions corresponding to bacteriopheophytin molecules in RC of purple bacteria [3,4], and two phylloquinone molecules (Q_A and Q_B).

Pairs of *Chl* and phylloquinone molecules are located in nearly symmetric electron-transport branches *A* and *B* and bound to subunits *PsaA* and *PsaB*, respectively. Branch A incorporates *ChlA1*, *ChlA2*, *ChlA3*,

and phylloquinone Q_A, whereas branch *B* incorporates *ChlB1*, *ChlB2*, *ChlB3*, and phylloquinone Q_B. The PS I electron-transport chain includes P700, A_0 (one or two dimers of molecules *Chl2A*/*Chl3A* and/or *Chl2B*/*Chl3B*), A_1 (one or two molecules of phylloquinone Q_A/Q_B), and iron–sulfur clusters F_X, F_A, and F_B. The problem of involvement of one or two symmetric branches of cofactors in electron transfer from P700* to F_X remains insufficiently understood [5–7].

In contrast to bacterial RCs, it is impossible to separate *Chl* molecules associated with PS I RCs from those belonging to light-harvesting antenna complex. This is accounted for by the fact that 90 antenna *Chl* molecules are attached to the same protein heterodimer *PsaA*/*PsaB* that carries also 6 *Chl* molecules constituting the initial part of the RC electron-transfer chain. These 96 *Chl* molecules also cannot be definitely distinguished by absorption spectral peculiarities. According to the literature [8], the main part of the antenna *Chl* pool has absorption maxima around 670–680 nm, while only a few *Chl* molecules (presumably dimers or trimers) are characterized by absorption in the 690–710 nm spectral region. Although it is generally accepted that the special pair *Chl* dimer P700 has its main absorption maximum around 700 nm, and *Chl* acceptor A_0 around 686 nm [9,10], they cannot be easily discriminated from several antenna *Chl* molecules that also absorb light in the same spectral regions. The exact absorption difference extremums were measured for the special pair P700 (~700 nm, 30 nm fwhm) and the primary acceptor A_0 (686 nm, 10 nm fwhm) [9,10].

In recent years, energy- and electron-transfer reactions in PS I have been studied using various ultrafast techniques, including pump–probe absorption spectroscopy (for review see [11]). However, the primary electron transfer reactions within PS I RC could not be clearly separated from excitation energy transfer since these reactions occur within the same time range. Several approaches have been used to separate electron transfer from energy transfer and to reveal the pure kinetics of primary electron transfer steps and the spectra of corresponding intermediates.

Kumazaki et al., 2001 [12] removed the majority of antenna *Chl* from the PS I RC and in these impaired complexes observed two kinetic components with time constants τ of ~0.8 and ~9 ps, which were ascribed to the primary charge separation. Note that the decrease in the total *Chl* content to 12–14 molecules most probably significantly changes both structure and functioning of the PS I complex.

There are two models describing charge separation in PS I. The first model suggests that upon absorbing a light quantum, the primary electron donor P700 goes into the excited state P700*, which is followed by the primary process of charge separation between P700* and primary acceptor A_0 with formation of $P^+A_0^-$ within <10 ps (see [7] for review). After that an electron is transferred within 50 ps to phylloquinone A_1 and then to cluster F_X within ≤200 ns.

The earlier work of Shuvalov et al. [13] demonstrated that selective excitation of PS I using 710-nm picosecond pulses led to the formation of the state $P700^+A_0^-$ with two bleaching bands at 700 nm (P700) and at 689 nm (A_0^-) within less than 10 ps, which decayed with time constant (τ) 21 ps. Another approach based on subtraction of the transient spectra of oxidized (closed) RCs from those of reduced (open) RCs was used in [14]. This approach eliminates spectral changes due to energy migration between *Chl* molecules in antenna and reveals spectral features accompanying electron transfer in the RC. It was suggested that antenna kinetics were essentially unaffected by the P700 oxidation state (see [11] for references). Hastings et al. [9] employed this approach for PS I particles from cyanobacteria and observed two main kinetic components with τ of 4 and 21 ps. These components were attributed to formation and disappearance of the primary radical pair $P700^+A_0^-$. They used unselective excitation at 590 nm, and therefore the 4-ps kinetics included not only oxidation of P700 but also energy transfer in antenna, and thus represented the upper limit for the kinetics of the formation of the primary radical pair. Moreover, to achieve reasonable signal/noise ratio in the $\Delta\Delta A$ difference ($\Delta\Delta A = \Delta A$(open) minus ΔA(closed) kinetic

signal), Hastings et al. [9] employed high-intensity laser pulses, which induced annihilation in the antenna and shortened the overall time for antenna equilibration. Savikhin et al. [15], using a similar approach, obtained the time constant of ~10 ps for the $P700^+A_0^-$ formation. They excited the sample at 660 nm with fwhm of ~100 fs under annihilation-free conditions. Later on, assuming a simple sequential model of electron transfer and using global fitting with two free parameters, Savikhin et al. [10] obtained the intrinsic time constants for $P700^+A_0^-$ formation and subsequent $A_0 \rightarrow A_1$ electron transfer of 1.3 and 13 ps, respectively. Similar results were obtained earlier by White et al. [16] in PS I complexes from spinach.

Melkozernov et al. [17], studying the fast spectral changes in PSI from the cyanobacterium *Synechocystis* sp. PCC 6803 excited by 150 fs pulses at 660, 693, and 710 nm came to the conclusion that an excitation wavelength-dependent ΔA around 700 nm most probably reflected the primary charge separation occurring in ~20 ps. They stated that their finding was more consistent with the trap-limited kinetic scheme in which equilibration processes in antenna were completed within ~3 ps and the rate-limiting step would be the conversion of $P700^*A_0$ to $P700^+A_0^-$. Note that other authors supported the alternative transfer-to-trap-limited model (see, for instance, [10,18,19]).

Gibasiewicz et al. [20,21] studied energy and electron transfer in PS I from *Chlamydomonas reinhardtii* excited at different wavelengths by 150 fs pulses at 20 K and room temperatures. They ascribed subpicosecond and 2–3 ps kinetic components to energy equilibration within the core antenna and ~20 ps component to energy trapping by RC [20]. The latter component was considered as reflecting the primary charge separation between P700 and A_0. However, no direct indications in favor of the latter statement were presented in this work. Chemical oxidation of the primary donor P700 did not change the transient spectrum at early delays at low temperature [21]. At room temperature, the spectra measured at 100 ps delay was not consistent with the spectrum of $P700^+$ measured by these authors with ms time resolution for the same PS I complex. Note that in the paper by Muller et al. [19] the transient spectrum at 300 ps delay for PS I from *Chlamydomonas reinhardtii* was very similar to the $P700^+$–P700 spectrum recorded on a millisecond time scale.

The second model for primary charge separation in PS I was suggested by Muller et al. [19]. These authors, studying PS I complexes from *Chlamydomonas reinhardtii* on the basis of kinetic compartment modeling and analysis of species-associated difference absorption spectra, suggested that the lifetime of the primary charge separation was 6–9 ps. They suggested that the primary charge-separated state might be not $P700^+A_0^-$ but $P700^+ChlA2^-$ or $ChlA2^+ChlA3^-$. In a recent paper, Holzwarth et al. [22] revealed three kinetic components with lifetimes of 3, 14, and 25 ps and suggested a scheme of the primary charge separation. This scheme implied $ChlA2^+ChlA3^-$ as primary reactants ($\tau = 3$ ps), while the slower components were attributed to formation of $P700^+ChlA3^-$ ($\tau = 14$ ps) and $P700^+A_1^-$ ($\tau = 25$ ps).

Summarizing the literature, we conclude that several important points still remain unclear, in particular, the nature of the primary electron donor and acceptor and the kinetics of the first, second, and (according to [22]) third radical pairs in PS I.

In this work we attempt to clarify these questions by excitation of PS I at the red edge of its Q_y band using 20 fs laser pulses centered at 720 nm. This approach was used to maximize the share of excited RC *Chls* in PS I.

2. Materials and methods

2.1. Sample preparation

Wild type *Synechocystis* sp. PCC 6803 cells were grown in BG-11 medium. Trimeric PS I complexes were isolated from thylakoids using n-dodecyl-β-D-maltoside (DM) and purified using sucrose gradient

ultracentrifugation as described in detail [23]. Samples were finally resuspended in 50 mM Tris–HCl (pH 8.0) buffer containing 0.03% (w/v) DM and 15% (v/v) glycerol at *Chl* concentration 1.5–2.0 mg mL^{-1}, and stored at −80 °C until required. The incubation mixture contained 50 mM Tris–HCl (pH 8.0) and 0.03% DM; the *Chl* concentration was 0.4 mg mL^{-1}. Experiments with open PS I RCs were performed in the presence of 10 mM sodium ascorbate and 4 μM 2,6-dichlorophenolin-dophenol (DCIP). To prepare "closed" RCs P700 was oxidized by illumination of the sample by cw laser with 10 mW at 532 nm, the light spot being of 6-mm diameter. The light beam was directed at 7° relative to the pump–probe beams (~3° between the latter). P700 was pho-tooxidized to P700^{+} in the absence of reductants (ascorbate and DCIP) so that the accumulation of A$_1^-$ state did not occur. The important criteria for photooxidation of P700 were the lack of the P700^{+} features in difference spectra at long delay (more than 50 ps). Two identical samples for open and closed states were used in short sequence.

2.2. Femtosecond laser photolysis setup

Transient absorption spectra were measured using a femtosecond pump–supercontinuum probe setup. The output of a "Tsunami" Ti: sapphire oscillator (800 nm, 80 MHz, 40 fs, Spectra-Physics, USA) was amplified by a "Spitfire" regenerative amplifier system (Spectra-Physics) up to 1 mJ/pulse at repetition rate 1 kHz. The amplified pulses were split into two beams. One half of the energy was directed into a non-collinearly phase-matched optical parametric amplifier. Its output centered at 720 nm with bandwidth of 40 nm (fwhm) was subsequently compressed by a pair of quartz prisms. The gauss pulse of 20 fs was used as a pump. The other half of the energy was focused into a quartz cell with H$_2$O to generate supercontinuum probe pulses. The pump and probe pulses were time-delayed with respect to each other by means of a computer-controlled delay stage. They were then attenuated, recombined, and focused into the sample cell with optical length to the spot of 100 μm. The pump pulse energy was attenuated at 20 nJ or to 50 nJ. The pump light spot had a diameter of 300 μm. The pump pulse repetition rate was 50 Hz. The relative polariza-tions of pump and probe beams were adjusted to 54.7° (magic angle). After the sample, the supercontinuum was dispersed by a poly-chromator (Acton SP-300) and detected by a CCD camera (Roper Scientific SPEC-10). Absorption difference spectra ΔA (t, λ), were recorded over the range 400–740 nm. The measured spectra were corrected for group delay dispersion of the supercontinuum using the procedure described previously [24]. The experimental data were treated using our own software programmed using MatLab®. The analysis of femtosecond transient absorption spectroscopy with chirped supercontinuum probing was performed according to the theoretical description of the recently developed method (see [25] and references therein). Particular attention was given to the "'coherence spike'" or "'coherent artifact'", which is observed at the beginning of the evolution during pump–probe overlap and which complicates the analysis of measurements. This "'coherence spike'" is caused by coherent interaction (for example, pump–probe–pump) of the electric field components with the material sample. The coherent contribution can be identified by its characteristic temporal behavior: it follows the pump–probe intensity cross-correlation and its time derivatives [25]. The detailed analysis of the PS I response in the region of the "coherent artifact" will be published elsewhere.

The experiments were carried out at 21 °C in a 0.45-mm flow optical cell with optical windows of 0.1-mm thickness. The circulation rate in the flow cell was fast enough to avoid multiple excitation of the same sample volume.

2.3. Global fitting and data treatment

The initial, intermediate, and product states are identified by their temporal behavior and SVD of ΔA (λ,t) is used to determine the

spectra associated with these photochemical species. Over the full spectral range we consider $M = 352$ equally spaced wavelengths from 410 to 730 nm and the delay time runs from 0.08 ps to 90 ps in 10 fs steps; hence, **A** is dimensioned $M \times N = 352 \times 8010$. By SVD the data can be written as $\mathbf{A} = \mathbf{U}(M \times L) \cdot \mathbf{S}(L \times L) \cdot \mathbf{V}^T(L \times N)$, where the columns of **U** represent normalized basic spectra, the rows of $\mathbf{V}^T$ contain their normalized dynamics, and diagonal **S** can be presumed to have the weights or singular values $S_{ll} > 0$ arranged in descending order. Usually just a few (say $K < L$) such combinations adequately describe the measurement; this is why after SVD the matrices **U**, **S**, and $\mathbf{V}^T$ are truncated to dimensions $M \times K$, $K \times K$, and $K \times N$, respectively. In our case $K = 3$ is sufficient.

3. Results

Fig. 1 shows the spectra of the laser flash-induced difference absorption changes in open PS I RCs (in the presence of ascorbate and low concentration of the redox dye (DPCIP) within the range from 400 to 730 nm at different time delays between actinic and monitoring flashes. The flash energy (20 nJ) was tuned to minimize the pro-bability of double excitation of individual RCs. It triggered only ~10% of the PS I RCs, but still provided acceptable signal/noise ratio. The spectrum at 85 fs delay reveals some specific features around the *Chl* Soret and Q$_y$ bands: bleaching bands at 440, 690, and 705 nm, a shoulder around 420 nm, and smaller developments between 460 and 500 nm and around 660 nm. This pattern represents the mixture of the *Chl* excited state properties and features previously ascribed to P700/P700^{+} and A$_0$/A$_0^-$ differential spectra [9,11,13,14,26–28]. Indeed, the 420, 440, 690 nm negative bands and 460–500, 660–670 nm positive bands were attributed to A$_0$/A$_0^-$, while 435, 680,
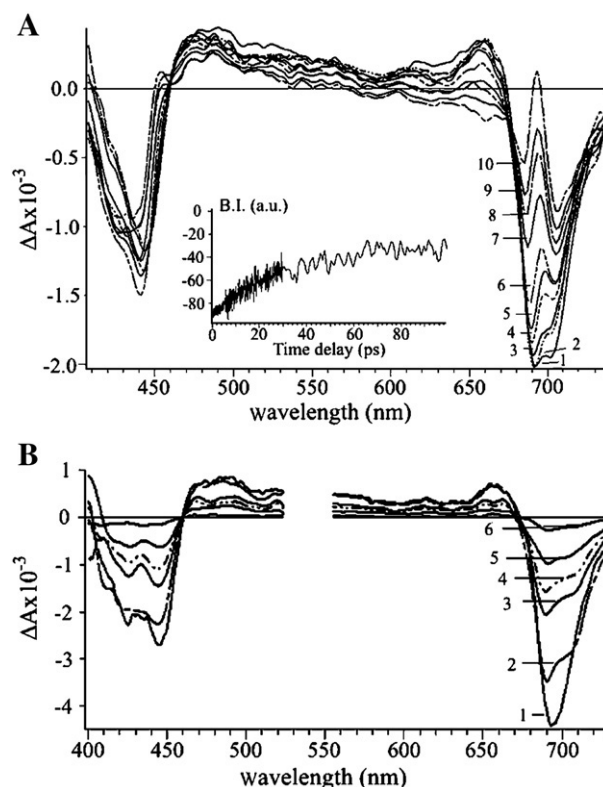
Fig. 1. Differential absorption spectra after excitation of PS I RCs from *Synechocystis* sp. PCC 6803 by 22 fs laser pulses centered at 720 nm. A. Open PS I RCs; excitation energy, 20 nJ. Time delay: 1) 85 fs; 2) 150 fs; 3) 500 fs; 4) 2 ps; 5) 4 ps; 6) 8 ps; 7) 20 ps; 8) 30 ps; 9) 50 ps; 10) 90 ps. B. Closed PS I RCs; excitation energy, 50 nJ. Time delay: 1) 100 fs; 2) 2 ps; 3) 11 ps; 4) 17 ps; 5) 32 ps; 6) 71 ps. The inset to the panel A shows the kinetics of band integral *BI* calculated in the range from 678 to 730 nm.

705 nm negative and 450, 465–500 nm positive bands to P700/P700$^+$ differential spectra.

At later delay until 2–4 ps these features are present without remarkable modification. Between 4 and 50 ps decrease in the bleaching bands at 690 and 705 nm in the difference spectra is observed. This effect is partially due to the replacement of the bleaching at 690 nm by a red shift of this band. At time delays longer than 50 ps the transient spectra presented in Fig. 1 demonstrate specific spectral features of P700$^+$: 1) in the region of the Q$_y$ band bleaching at 686 and 705 nm with development at 694 nm; 2) bleaching at 439 nm corresponding to the Soret band; 3) a sharp peak at 453 nm and broad positive band between 465 and 580 nm; 4) a very small negative motif between 580 and 670 nm; and 5) isobestic points at 579, 449, and at 420 nm.

Note that the steady-state difference (reduced minus oxidized) spectrum of PS I is similar to the spectrum obtained by 20 fs laser pulse excitation at 95 ps delay (see supporting information). Fig. 1B shows transient spectra for closed PS I RCs (P700 was initially oxidized). The spectra of closed RCs were prepared by additional continuous illumination at 532 nm in the absence of reductants (ascorbate and DCIP). In this case, the energy of the laser flash was increased up to 50 nJ to increase the signal/noise ratio for further comparison of the open and closed PS I transient spectra (see Fig. 3 below).

The main spectral features typical of the open PS I RCs (Fig. 1A) were not observed in closed PS I RCs (Fig. 1B). Comparison of the spectra presented in Fig. 1A and B demonstrates significant differences.

1. The earlier ΔA spectra of the open RCs in the Q$_y$ band are characterized by a bleaching band at ~690 nm, which is shifted to 685 nm within ~100 ps, while the similar bleaching in the spectrum of the closed RCs remains virtually unshifted. The shoulder observed between 695 and 710 nm after 2 ps delay for closed RCs is considerably different from the clearly resolved minimum at 705 nm of P700$^+$ observed for the open RCs after 90-fs delay. This is accompanied by the development at 694 nm at later delays for open RCs.
2. The shape of the early transient spectrum of the closed RCs in the Soret region has a pronounced bleaching at 425 nm that is not observed in the spectrum of the open RCs. In contrast to closed RCs, where the main bleaching in the Soret band is observed at 444 nm and remains unshifted until 100 ps, in the open RCs the band at 441 nm shifts to ~437 nm within 100 ps.
3. The spectrum of the closed RCs in the range from 460 to 640 nm also differs from that in open RCs by the absence of the dip at 465 nm and of the bleaching of the broad band at 650–670 nm at long delays.

To discuss the question concerning a part of the excitation energy absorbed by RCs and converted to the charge-separated state (P700$^+$A$_0^-$), the band integral of the bleaching interval of 678–730 nm was analyzed. The band integral (BI) of the bleaching reveals the absorption of Chl molecules excited by the 720-nm pulse. The BI is defined as $BI = \int_{v_1}^{v_2} \frac{\Delta Abs(v)}{v} \cdot dv$ (where $v1$, $v2$ correspond to 678 and 730 nm, respectively). There is a decrease in the BI value by a factor of ~2.25 from 80 fs to 90 ps (Fig. 1, inset). The value of the decrease roughly corresponds to one-half loss of the Chl dipole strength, which agrees with the common view that the primary radical pair consisting of the Chl cation- and anion-radicals during this time range turns into the secondary radical pair consisting of the Chl$^+$ cation radical and A$_1^-$ semiquinone.

Fig. 2A demonstrates the detailed set of kinetic spectra between 0 (zero time between pump and probe laser pulses) and 100 fs. Fig. 2B shows the steady-state absorption spectrum of PS I (left y-axis) and the spectrum of the 20-fs laser pulse (right y-axis). The product of these two normalized spectra is presented in Fig. 2A as a dotted line. This product is characterized by a maximum at 691 nm and fwhm of
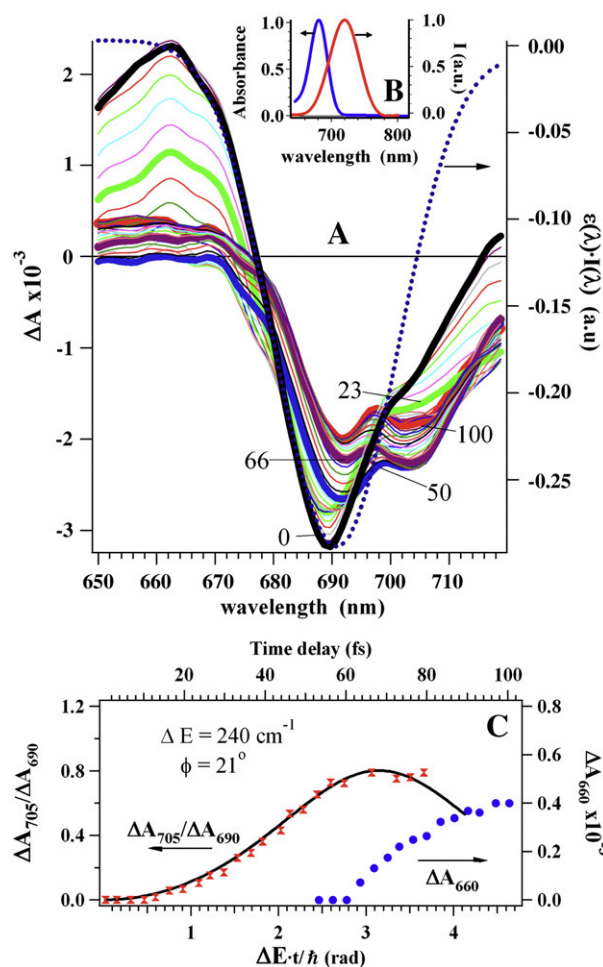

Fig. 2. The earliest events observed in open PS I RCs around the Q$_y$ band. A) Differential absorption spectra evolution in the 0–100 fs time domain; excitation energy, 20 nJ. Evolution of spectra is shown with time delay step of 3.33 fs. Spectra with time delays 0 fs, 23 fs, 50 fs, 66 fs and 100 fs are shown by tags (left axis). The dotted line represents the inverted overlap between absorption spectrum of PS I ε(λ) and the spectrum of the excitation pulse I(λ) (right axis). B) Absorption spectrum of PS I RCs at the Q$_y$ band (left axis) and normalized laser pulse spectrum (right axis). C) Kinetics of the ratio of differential absorption ΔA$_{705}$/ΔA$_{690}$ (left axis, experimental points are shown by hourglass symbol, solid line is a theoretical curve simulated by the quantum-mechanical mixing of two excited energy levels defined by expression 6 in the Discussion) and kinetics of differential absorption of ΔA$_{660}$ after 60 fs (right axis, filled circles).

25 nm and reflects the efficiency of the light absorption by PS I upon a 20-fs excitation pulse centered at 720 nm. The shape of the bleaching centered at 690 nm of PS I at zero delay is very close to the shape of that product spectrum, showing dynamic hole burning when the bleaching is not broadened and the energy is not transferred to other chromophores at early delays. In other words, the Chl molecules that become primarily excited are the molecules that have maximal absorption coinciding with the product spectrum. The visible deviation of the zero delay spectrum from the product spectrum at wavelengths longer than 700 nm probably reflects the direct excitation of the red-most Chl molecules (including P700). The zero delay spectrum includes intensive absorption development in the range from 650 to 680 nm, which can be attributed to the primary excited state of PS I. This development is decreased to 0 within 50 fs.

At delays longer than 10 fs energy transfer occurs with a decrease in the bleaching at 690 nm and appearance of additional bleaching at 705 nm. These changes are observed in the time range from ~10 to 60 fs (Fig. 2C). Fig. 2C demonstrates the kinetics of increase in the ratio ΔA$_{705}$/ΔA$_{690}$ (circles). In the range from 0 to 70 fs this ratio is developed according to the quantum oscillation formalism (Fig. 2C,

solid line) representing the ratio of populations $|c_2|^2/|c_1|^2$ proportional to $\Delta A_{705}/\Delta A_{690}$ (see Eq. (6) for definitions).

However, at time intervals longer than 80 fs a deviation of the experimental points from the theoretical curve is observed showing almost equal distribution of the excitation energy between 690-nm and 705-nm chromophores (the ratio $\Delta A_{705}/\Delta A_{690}$ remains ~0.8 in the time range from 85 fs to ~8 ps in agreement with Fig. 1). The ~50%-distribution between P700* and A_0^* is accompanied by a loss in the 660-nm band of the excited state at 50 fs delay (Fig. 2A). This shows that the femtosecond excited state distribution between A_0 and P700 is probably related to the electron density distribution (~50/50) between LUMO and HOMO orbitals of the chromophores. At the 60-fs delay the development of the new 660-nm band starts; this development is completed within the next 40 fs. The band at 660 nm decays with the time constant ~26 ps simultaneously with bleaching decay at 694 nm reflecting the electron transfer from A_0^- to A_1, which results in the formation of the pure P700$^+$ spectrum with the maximum at 705 nm (see below Fig. 3B and D). Taking into account the spectrum of reduced *Chl* in solution [29], it is safe to ascribe the band at 660 nm to formation of *Chl* anion radical (most probably to A_0^- with the main bleaching at

690 nm). The formation of the new 660-nm band typical to *Chl* anion radical is a direct indication in favor of very fast (within 100 fs) formation of the primary radical pair P700$^+$A$_0^-$. Additional evidence for the formation of the state P700$^+$A$_0^-$ within 100 fs is a significant difference in the dynamics of the 660-nm band for open and closed RCs. At ~0 fs time delay this band is similar for the two states (not shown for the closed state). However, in open RCs it decreases to zero at 50 fs, then increases again within the next 40 fs (Fig. 2A), while in closed RCs this band gradually decreases within 100 ps (Fig. 1B).

Because the ratio $\Delta A_{705}^{100}/\Delta A_{690}^{100}$ at 100 fs is ~0.8 (Fig. 2A), it is safe to suggest that under the conditions of the experiment the femtosecond excitation leads mainly to the formation of A_0^* at 0 fs and of P700$^+$A$_0^-$ at 100 fs delay. In this case, the ratio $(\Delta A_{690})/(\Delta A_{690}+\Delta A_{705})$ should be equal to 0.55. This value could reflect the ratio between ΔA corresponding to A_0^* at 0 fs and the sum of ΔA corresponding to P700$^+$ and A_0^- at 100 fs delay. However, the experimentally determined ratio $(\Delta A_{690}^0)/(\Delta A_{690}+\Delta A_{705})$ is 0.76 (data taken from Fig. 2A). This discrepancy is probably related to the excitation of antenna *Chl* at 0 delay in addition to the formation of A_0^*. We estimated the value of initial excitation distribution between A_0^* and An* corresponding to the experimentally observed ratio $(\Delta A_{690}^0)/(\Delta A_{690}^{100}+\Delta A_{705}^{100})$ equal to 0.76. The estimation showed that this ratio fitted with ~50% distribution between directly excited RC and the *Chl* species in antenna.

As mentioned in the Introduction, to reveal the oxidation of P700 to P700$^+$ and reduction of A_0 to A_0^-, two strategies were employed: (i) selective excitation of P700 and (ii) subtraction of the transient spectra of oxidized (closed) RCs from those of reduced (open) RCs. As discussed before, the femtosecond excitation centered at 720 nm with energy of 20 nJ leads to the excitation of RC pigments and charge separation within less than 100 fs. The excitation of antenna absorbing in the same spectral range was studied using femtosecond pulses centered at 720 with 50 nJ to increase the signal/noise ratio.

For this case the subtraction of the transient spectra of oxidized (closed) RCs from those of reduced (open) RCs gives additional information. As it was demonstrated [16], the subtraction procedure should eliminate spectral changes due to energy migration between *Chl* molecules in antenna and reveal spectral features accompanying electron transfer in the RC. It should also eliminate any charge separation within RC pigments in the presence of P700$^+$. It is suggested that antenna kinetics are essentially unaffected by the P700 oxidation state (see [11] for references). It should be noted that the excitation of the antenna (An) *Chl* induced at early delays should be very similar for open and closed RCs regardless of possible decay kinetics differences at later delays, because all fast processes in the antenna are evidently independent of the state of P700. This is also relevant to the suggested primary charge separation between ChlA2 and ChlA3 (20).

Fig. 3 shows the subtracted (open minus closed, $\Delta\Delta A$) difference absorption spectra at early (90 fs–1.5 ps, Fig. 3A) and later (3–80 ps, Fig. 3B) delays between pump and probe laser pulses. Note that in Fig. 3 the closed spectra were subtracted from the open spectra without normalization of ΔA amplitudes. The most interesting feature observed at the Q_y band upon excitation centered at 720 nm is the appearance of two narrow bleaching bands centered at 705 and 689 nm at early delays, accompanied by the development at 660 nm. In agreement with 20-nJ experiments (Figs. 1A and 2) these features can be attributed to the formation of P$^+$A$_0^-$.

The band at 705 nm can be tentatively ascribed either to formation of excited state P700* or to the oxidation of P700 forming P700$^+$, while the band at 690 nm can be ascribed either to formation of A_0^* or to reduction of A_0 to A_0^-. These features are observed at very short delay (96 fs) and even near zero delay between pump and probe (not shown). The possibility of observing A_0^* in the $\Delta\Delta A$ spectra at 96 fs is very unlikely since A_0^* should exist both in open and closed RC and should be subtracted in $\Delta\Delta A$ (open minus closed) spectra (see Fig. 3A). The same argument can be applied to the possibility of the
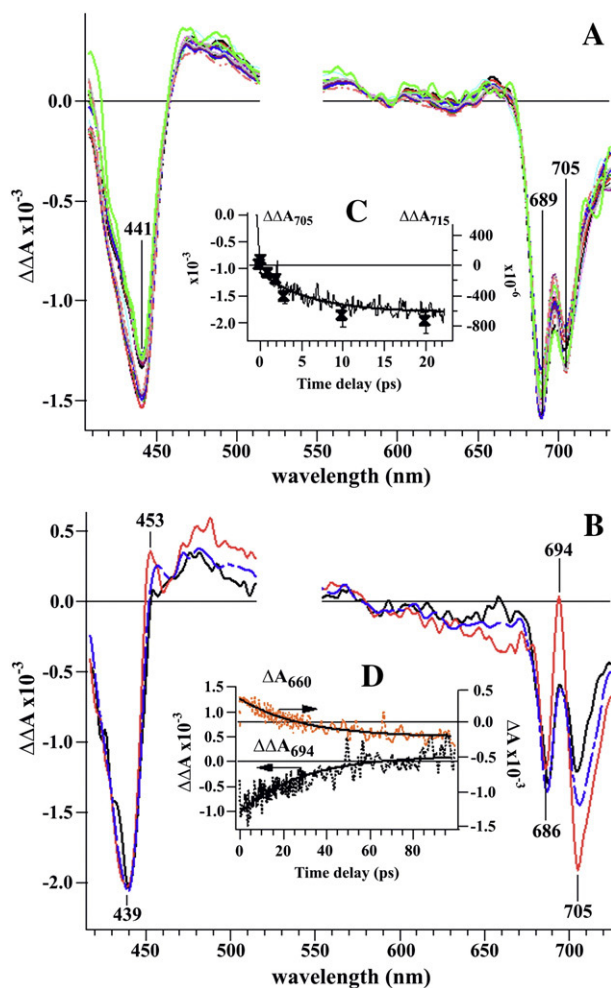

Fig. 3. $\Delta\Delta A$ is the difference between open and closed spectra of PS I RCs; excitation energy, 50 nJ. A) Transient spectra for time delays between 90 fs and 1.5 ps. B) Transient spectra for 3 ps (black), 12 ps (blue) and 80 ps (red) delays. C) Kinetics of $\Delta\Delta A$ at 705 nm for open PS I RCs is represented by the solid line (left axis), and kinetics of $\Delta\Delta A$ at 715 nm for closed PS I RCs, shown by hourglass symbols, were taken from Fig. 4A (right axis). Approximation using exponential fitting gives τ ($\Delta\Delta A_{705}$) = 5.7 ± 0.4 ps, $\tau(\Delta\Delta A_{715})$ = 4.5 ± 0.8 ps. D) Kinetics of $\Delta\Delta A$ at 694 nm corresponds to the left axis and ΔA at 660 nm corresponds to the right axis (the latter data were taken from the experiment with open PS I RCs at 20 nJ excitation).

formation of the state $A_2^+ A_3^-$ (22). Therefore, early delay $\Delta\Delta A$ spectra are most probably related to the formation of $P^+A_0^-$.

Fig. 3C demonstrates two kinetic components at 705 nm monitoring the appearance of P700$^+$. The first component is developed within less than 100 fs (~60%); the second, within ~5 ps (~50%). In agreement with 20-nJ experiments the first component is due to charge transfer in RCs, in which six excitonically coupled *Chl* molecules (*A1, A2, A3, B1, B2* and *B3*) are directly transformed into one photon-excited state. The second component seems to reflect the energy transfer from An* to RC pigments that were not excited directly by the femtosecond pulses.

In the framework of our model, the excitation energy transfer (~5 ps) is much slower than the primary charge separation (<100 fs). Thus, the energy transfer from An* to P700 can be considered as almost irreversible. Fig. 3D shows the kinetics of the electron transfer from A_0^- to A_1 with time constant ~26 ps (see the data given below for SVD analysis).

The detailed consideration of the flash-induced transient spectra of the open and closed RCs in the 705–730 nm spectral region shows that the bleaching is more pronounced in the closed than in the open RCs. To reveal this difference, all spectra were normalized to the value of the transient absorbance at 705 nm (Fig. 4). This wavelength was chosen on the basis of the fact that the maximal bleaching due to P700$^+$ formation was observed at 705 nm. Therefore, this normalization procedure eliminates the main bleaching absorption band and highlights the possible stimulated emission. Further the transient spectrum observed at the time delay of 90 fs was subtracted from the spectra observed at all other time delays. The latter procedure was performed so as to eliminate from the negative transient spectra the bleaching signal and to enhance the amplitude of the stimulated emission.

Fig. 4 demonstrates the transient spectra obtained using the procedure described above for closed (4A) and open (4B) RCs. The observation of the bleaching in the range of 705–725 nm for closed RCs can be due either to "red" pigment bleaching or to the stimulated emission centered at 715 nm. It is lacking in the case of open RCs. The bleaching in this spectral range was previously ascribed to energy transfer between antenna *Chl* molecules [30]. In our opinion, in the case of closed RCs (Fig. 4A) the bleaching centered around 715 nm most probably reflects the energy transfer in antenna that is not quenched by P700 since P700 is oxidized to the state P700$^+$ by continuous illumination. On the other hand, the lack of emission in this region in the case of open RCs demonstrates the very effective quenching of the *Chl* excited states and supports the concept of very

fast (<100 fs) formation of P700$^+$A$_0^-$ state upon excitation at 720 nm. Remarkably, the development of the bleaching at 715 nm in closed RCs coincides roughly with 5-ps oxidation of P700 in open RCs. This is evident from the data presented in Fig. 3C, where several points reflecting the kinetics of the 715-nm (hourglass symbol) bleaching in closed RCs (taken from Fig. 4A) and the kinetics of the $\Delta\Delta A$ bleaching at 705 nm in open RCs were superimposed. This observation can be considered as an indication in favor of similarity of energy transfer rates in open and closed RCs under the given conditions.

4. Discussion

4.1. Evidence for very fast P700$^+$A$_0^-$ formation

From the description of Figs. 1–4 there are several indications in favor of the formation of P700$^+$A$_0^-$ rather than (P700A$_0$)* within less than 100 fs upon excitation of PS I by femtosecond pulses centered at 720 nm. The main evidences and other important features can be summarized as follows:

1) Negative bands around 440 and 690 nm and positive bands near 470 and 660–670 nm (Figs. 1A and 3A) are characteristic for the formation of *Chl* anion radical in DMF [29] and for the (A_0^- – A_0) difference spectrum in PS I [9,13,26,31]. Therefore the formation of these characteristic features, and in particular of the 660 nm band attributed to the anion radical of a *Chl* molecule [26] in less than 100 fs (Fig. 2C), is a direct indication in favor of the appearance of the P700$^+$A$_0^-$ state.

2) The bleaching centered at 690 nm and observed at 0 time delay between the pump and probe laser pulses decreases simultaneously with the appearance of the additional bleaching at 705 nm within ~70 fs (Fig. 2A and C). The ratio between absorbance negative bands at 705 and 690 nm ($\Delta A_{690}/\Delta A_{705}$) increases within ~70 fs (Fig. 2B) and remains virtually unchanged up to ~8 ps (Fig. 1A). These dynamics are consistent with the hypothesis of the primary charge-separated state P700$^+$A$_0^-$ appearing within less than 100 fs.

3) The bleaching band at 690 nm probably does not correspond to A_0^* at delays from 90 fs to 1.5 ps because the subtraction of the transient spectra of closed RCs from those of open RCs should almost completely eliminate the signal of A_0^* in the difference spectra, which contradicts the experimental data (Fig. 3A). The possible influence of the P700$^+$ state induced by continuous illumination on the A_0^* spectrum can be only related to a small red shift of A_0 ground state absorption. The presence of the intensive bleaching at 690 nm at short delays can be hardly attributed to a short-wavelength transition of P700*, because the orientation of dipole transition moments of monomers in P700 is similar to those in bacterial reaction center (BRC), which are characterized by allowed long-wavelength transition and forbidden short-wavelength transition.

4) The wide positive band centered at ~660 nm and observed at 0 time delay decreases within ~50 fs and then increases again to a lower level during the next 40 fs (Fig. 2A and C). These dynamics can be attributed to the immediate formation of A_0^* state, subsequent energy redistribution between A_0^* and P700*, and further $A_0^{\delta*}P700^{\delta*} \rightarrow P700^+A_0^-$ transition. This hypothesis is substantiated by the following behavior of the 660-nm band: it remains unchanged within several picoseconds and then decreases with time constant of 26 ps (Fig. 3D). The kinetics of the ΔA_{660} decay are similar to the kinetics of the ΔA_{694} decay. This decay is representative of the P700$^+$A$_0$A$_1$ → P700$^+$A$_0$A$_1^-$ transition observed as a red shift of the 690-nm band during P700$^+$ formation. In agreement with this result, the time constant of 25–30 ps for $A_0 \rightarrow A_1$ electron transfer was reported in a recent work by Giera et al. [32]. The main difference between the excited state
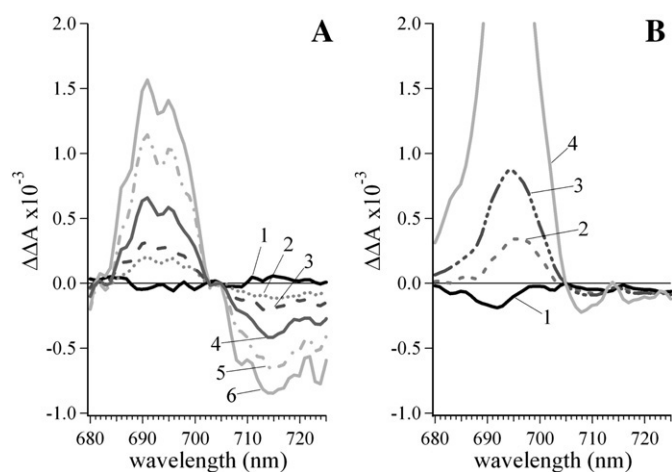

Fig. 4. $\Delta\Delta A$ is the difference between transient spectra ΔA (t) and ΔA ($t = 60$ fs). A) $\Delta\Delta A$ is shown for closed PS I RCs. Time delays: 1) 240 fs; 2) 1 ps; 3) 2 ps; 4) 3 ps; 5) 10 ps; 6) 20 ps. B) $\Delta\Delta A$ is shown for open PS I RCs. Time delays: 1) 200 fs; 2) 1.2 ps; 3) 2.5 ps; 4) 29 ps.

of Chl (most probably A_0^*) and Chl anion (A_0^-), which both can be characterized by a development at 660 nm, is a tremendous gap between the time constants of decay kinetics: 50 fs an 26 ps, respectively. It is unlikely that the 660-nm band lifetime of 26 ps reflects any excited state in RC since in this case Chl* should be directly converted to Chl^+ ($P700^+$) and A_1^-.

5) A significant difference between the transient spectra of open and closed RCs is observed in the whole spectral range both at early and late delays (Fig. 1). In particular, the bleaching at 705 nm characteristic of $P700^+$ formation appears in open RCs within 100 fs, while for closed RCs the shoulder between 695 and 710 nm forms in the picosecond time range. The latter process could be ascribed to energy transfer in antenna from the *Chl*-690 to the red-most *Chl* species when P700 is oxidized. The difference between open and closed PS I RC transient spectra reveals the spectral features attributed to the $P700^+A_0^-$ state (Fig. 3A) and to the $P700^+A_1^-$ state (Fig. 3B, red curve with 694-nm positive development). The latter state represents almost pure spectrum of $P700^+$, because phylloquinone anion A_1^- spectral features are only revealed in the near-UV spectral region. It is important that the difference transient spectra presented in Fig. 3 are very similar to the transient spectra of the open PS I RCs (Fig. 1A). This similarity includes the position of bleaching minima both in the Q_y and Soret bands, the value of ratio $\Delta A_{690}/\Delta A_{705}$ at early delays, and the dip at ~465 nm typical of $P700^+$ spectra at late delays.

6) Fig. 4 evidences the fast excited *Chl* quenching in the open RCs and supports the concept of very fast formation of the $P700^+A_0^-$ state. The registration of the 715-nm bleaching in closed and its absence in open RCs points out the very effective quenching of excitation under energy transfer to P700 in the open RC.

Effective quenching suppressing 715-nm bleaching by more than a factor of 10 indicates that the intrinsic time constant τ of charge separation between P700 and A_0 is <0.5 ps (τ of energy transfer from antenna to P700 in open RC is ~5 ps, see Fig. 3C). This result corroborates the assumption that the spectra at very early delays presented in Figs. 2A and 3A represent the charge-separated state $P700^+A_0^-$, rather than excited state $(P700A_0)^*$. Otherwise, the 90-fs spectrum would differ from the 1.5 ps spectrum, as the former would reflect the state $(P700A_0)^*$, while the latter would reflect $P700^+A_0^-$ (Fig. 3A).

The resemblance of the kinetics of the 5-ps bleaching at 705 nm in open RCs and 715-nm kinetics in closed RCs (Fig. 3C) reveals the similarity of the energy transfer from An* (mostly antenna *Chl* absorbing around 690 nm) to P700 in open RCs and to the red *Chl* in closed RCs. The excitation of the red *Chl* should lead to the bleaching or emitting in the range 705–715 nm. This shows the identity of energy transfer in open and closed RCs.

7) Fig. 3C demonstrates kinetics of $\Delta\Delta A_{705}$ that reveal two main processes in PS I upon excitation by femtosecond pulses: i) "immediate" excitation of RC pigments (~50%) with very fast (<100 fs) formation of $P700^+A_0$ and ii) energy transfer from An* to P700 within 5 ps. The first process is definitely due to the charge transfer in RCs, in which six excitonically coupled *Chl* molecules (*A1*, *A2*, *A3*, *B1*, *B2* and *B3*) are directly transformed into one photon-excited state. The second process seems to reflect the energy transfer from An* to RC pigments that were not excited directly by the femtosecond pulses.

8) The preferential excitation of antenna *Chl* by femtosecond laser pulses centered at 680 and 700 nm results in formation of much more developed bleaching at 685 nm that masks the smaller 705 nm bleaching band, which is characteristic of $P700^+$ (not shown, manuscript in preparation). In this case the formation of the primary radical pair $P700^+A_0^-$ in the picosecond time domain is mainly limited by the excitation energy transfer within the light-harvesting antenna complex.

4.2. Global fitting analysis of the transient spectra

According to the evidence presented above, the main events in PS I RCs can be summarized by Scheme (1):

$$An^* \xrightarrow{k1} \left((PA_0)^*A_1 \xrightarrow{<100\,fs} P^+A_0^-A_1 \right) \xrightarrow{k2} P^+A_0A_1^-. \tag{1}$$
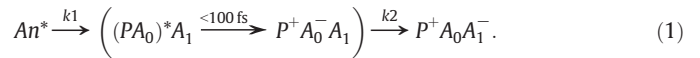
The initial conditions after excitation by ~20-fs laser pulses centered at 720 nm are: the population of $An^*|_{t=0} = \alpha$ and the population of $P^*A_0A_1|_{t=0} = 1 - \alpha$, where $0 \le \alpha \le 1$. For the particular case of excitation at 720 nm revealed from Fig. 2C, $\alpha = 0.5 \pm 0.1$.

Due to fast conversion $(PA_0)^*A_1 \xrightarrow{<100fs} P^+A_0^-A_1$, Scheme (1) can be simplified to Scheme (2):

$$An^* \xrightarrow{k1} P^+A_0^-A_1 \xrightarrow{k2} P^+A_0A_1^-, \tag{2}$$

where $P^+A_0^-A_1|_{t=0} = 1 - \alpha$.

The kinetic equations related to Scheme (2) for the state populations $K[An^*]$, $K[P^+A_0^-A_1]$, and $K[P^+A_0A_1^-]$ have the following solution:

$$K[An^*] = \alpha \exp(-k1 \cdot t)$$

$$K\left[P^+A_0^-A_1\right] = \left\{ 1 + \alpha \cdot \frac{k2}{k1-k2} \right\} \exp(-k2 \cdot t) - \alpha \cdot \frac{k1}{k1-k2} \exp(-k1 \cdot t)$$

$$K\left[P^+A_0A_1^-\right] = 1 + \alpha \cdot \frac{k2}{k1-k2} \exp(-k1 \cdot t) - \left\{ 1 + \alpha \cdot \frac{k2}{k1-k2} \right\} \exp(-k2 \cdot t).$$

To perform singular value decomposition (SVD), the experimental data can be represented by the following expression:

$$\Delta A(t, \lambda) = \Sigma_{i=1}^3 K_i(t) S(\lambda)_i, \tag{3}$$

where $S(\lambda)_i$ are the spectra of individual states i (An^*, $P^+A_0^-A_1$, and $P^+A_0A_1^-$) and $K_i(t)$ is the population of the states at different times.

To find $k1$ and $k2$ values as well as to reveal spectra of these states and kinetics of transitions between An^*, $P^+A_0^-A_1$, and $P^+A_0A_1^-$ the experimental data related to open PS I were analyzed using the global fitting procedure according to Scheme (2). The technique of SVD of the data matrix was applied to the global fitting analysis. The algorithm of global fitting for the femtosecond experiment is described in [33]. The data of experiments with the pump pulse energy of 20 nJ and 50 nJ were used for the analysis. A reasonable coincidence of the rate constants $k1$, $k2$, spectra $S(\lambda)$ and kinetic profiles $K(t)$ of An^*, $P^+A_0^-A_1$, and $P^+A_0A_1^-$ states was obtained from the fits of these data.

This analysis, in addition to considerations mentioned above, shows that multiexcitation processes are negligible in the present experiments. The obtained best fit rate constants were $k1 = 0.19 \pm 0.04$ ps^{-1} and $k2 = 0.038 \pm 0.007$ ps^{-1}, which correspond to the characteristic time constants $\tau1 = 5.3$ ps and $\tau2 = 26$ ps, respectively. The results of global fitting are shown in Fig. 5. The spectra of the states An^*, $P^+A_0^-A_1$, and $P^+A_0A_1^-$ states are shown in the left panels (A1, B1, and C1). The population kinetics of the states An^*, $P^+A_0^-A_1$, and $P^+A_0A_1^-$ are depicted in the right panels (A2, B2, and C2). It can be easily demonstrated that the populations of excited states at early delays in RC pigments and in An *Chl* are approximately equal. The experimental data matrix $\Delta A(t, \lambda)$ is well approximated by the sum of products of spectra in the left panels multiplied by population kinetics in the right panels.

The calculated spectra presented in Fig. 5 (panels B1 and C1) coincide very well with the experimental spectra (obtained by subtraction of the spectrum of closed from the spectrum of open
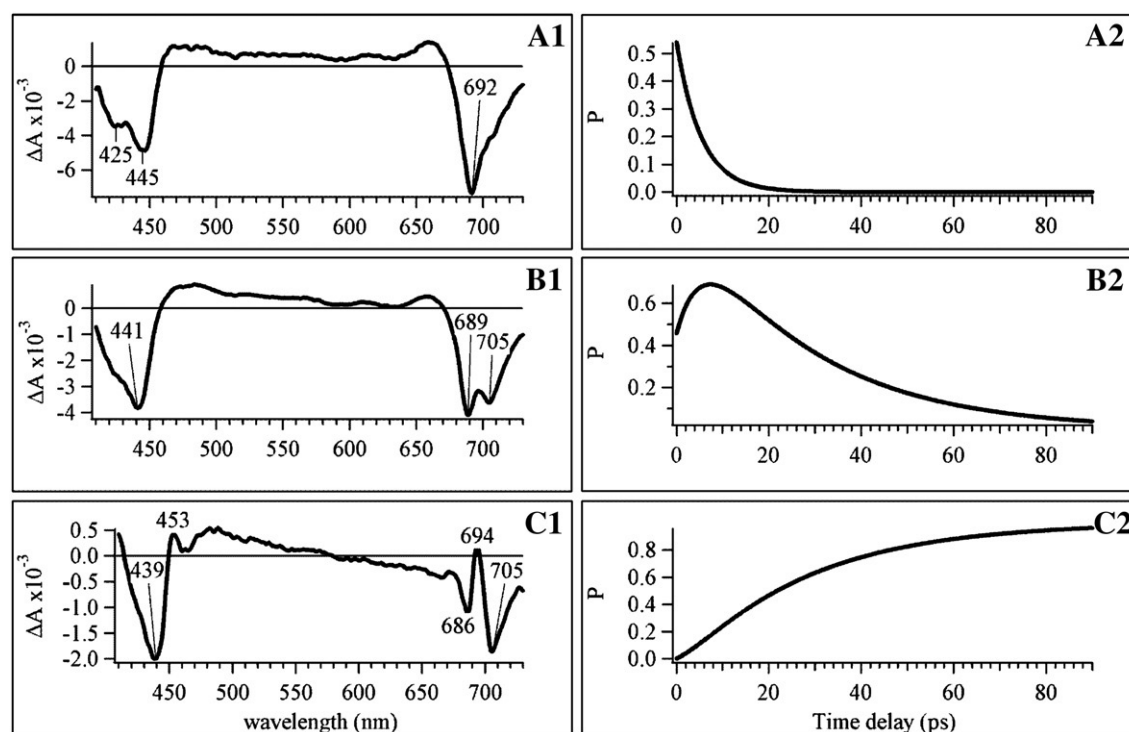
Fig. 5. Formation and decay of intermediate states revealed by the global fitting analysis using SVD of the data matrix. The left column represents the spectra of intermediate states: A1) An*; B1) $P^+A_0^-A_1$; C1) $P^+A_0A_1^-$. The right column shows the kinetics of formation and decay of intermediates: A2) decay of An*; B2) formation and decay of $P^+A_0^-A_1$; C2) formation of $P^+A_0A_1^-$.

RCs) presented in Fig. 3A and B. It is significant that in both cases the peaks of the bleaching and developments are identical.

4.3. Structural and thermodynamic considerations

It was previously believed that either one or both molecules (Chl3A and Chl3B) distal to P700 Chl constitute A_0. However, mutual arrangement (almost parallel planes of porphyrin rings) and relatively close distance between central Mg^{2+} atoms of Chl2A and Chl3A, as well as Chl2B and Chl3B (8.7 and 8.2 Å, respectively), imply the possibility of significant interaction between these pairs of Chl molecules. This allows considering A_0 as a Chl2A/Chl3A (or Chl2B/Chl3B) dimer. The distances between the monomers in these dimers are longer than in P700, and the asymmetry in the energy of monomer interaction with surrounding protein is much higher than in P700. Therefore, these dimers can be considered as looser. Recently, the midpoint redox potential (E_m) values of all 6 Chl molecules forming the initial part of the redox cofactors chains in PS I RCs were calculated [2]. It was demonstrated that consideration of Chl2A/Chl3A (Chl2B/Chl3B) as a dimer produces a ~50 mV positive shift of the reduction potential of the A_0/A_0^- pair (as compared to the monomers Chl3A (3B)). The energy of 700 nm quanta is 1770 mV. Taking into account the midpoint redox potential (E_m) value of the $P700/P700^+$ transition (+450 mV), the redox potential of P700 in its excited state ($P700^*$) is −1320 mV. Comparison of this value with calculated E_m values of A_0 (if the latter is represented by Chl3A or Chl3B) shows that the ΔG value between $P700^*$ and A_0/A_0^- falls within the range −5 to −50 mV [2]. On the other hand, if A_0 is considered as a dimer, the energy gap would increase up to −55 to −105 mV. This value is significantly lower, but closer to the 250 mV estimation of the value of ΔG between $P700^*$ and A_0/A_0^- based on delayed fluorescence measurements [34]. It should be noted that consideration of monomeric Chl2A(2B) as a primary acceptor is fairly unrealistic because its reduction potential is ~110 mV more negative than that of the $P700^*$ excited state [2].

Recently Holzwarth et al. [22] suggested that the Chls of the P_A and P_B pair (Chls1A/1B), constituting the primary electron donor P700, were not oxidized in the first electron transfer step, and they rather served as a secondary electron donor. They suggested that the accessory Chls (designated as Chl2A and Chl2B) functioned as primary electron donor(s) and Chls 3A and 3B (also called A_0) were the primary electron acceptor(s). To test this hypothesis, we calculated the oxidation midpoint potentials of the Chl2A and Chl2B species [2]. It was shown that the E_m values of Chl2A/Chl2B were ~60 mV more positive, than the values of reduction potentials of the hypothetical primary acceptor(s) Chl3A/Chl3B. Thus, the electron transfer between Chl2A(2B) and Chl3A(3B) is thermodynamically unfavorable, and, therefore, the functioning of accessory Chls 2A(2B) as primary donor seems unlikely.

In the present work we obtained some additional spectral indications that contradict the concept of accessory Chl2A/2B functioning as the primary donor. In fact, the data presented in Fig. 2A indicate almost immediate (<100 fs) appearance of the bleaching at 705 and 690 nm, which we ascribed to $P700^+A_0^-$ radical pair formation. The bleaching at 705 nm can hardly be attributed to the monomeric Chl species. Thus, to ascribe the role of the primary donor to Chl2A (Chl2B), one should postulate the formation of $Chl2A^+$ to be faster than $P700^+$ (<100 fs). This assumption seems to be very unrealistic.

4.4. Possible mechanism of the ultrafast primary charge separation

The primary bleaching at 0 time delay is observed for those molecules that have maximal absorption coinciding with the product of absorbance and pulse spectra at 690 nm (Fig. 2A). At delay times longer than 10 fs the energy transfer occurs with a decrease in the bleaching at 690 nm and an appearance of additional bleaching at 705 nm. This process starts from the first 10 fs and develops up to 60 fs (Fig. 2C). It appears to create the Frenkel exciton within RC pigments.

Fig. 2C demonstrates the kinetics (circles) of the ratio $\Delta A_{705}/\Delta A_{690}$ nm. In the range from 0 to 80 fs this ratio can be modeled by the quantum beat formalism. This formalism is based on the quantum-mechanical mixing of two excited energy levels of chromophores in aggregate with ψ_1 (E_1) and ψ_2 (E_2). In the case under consideration, ψ_1 (E_1) and ψ_2 (E_2) are related to the excited states of A_0^* and P700*, respectively. They are mixed giving new wave-functions Ψ_S and Ψ_A with energies E_S and E_A, respectively (see [35] and [36]):

$$\Psi_S = \{\cos\phi\,\psi_1 + \sin\phi\,\psi_2\}\exp\{-(i/\hbar)E_St\},$$

$$\Psi_A = \{\cos\phi\,\psi_2 - \sin\phi\,\psi_1\}\exp\{-(i/\hbar)E_At\}, \qquad (4)$$

where

$$E_{S,A} = (E_1 + E_2)/2 \pm 0.5\sqrt{\{(E_1-E_2)^2 + 4V_{12}^2\}},$$

$$tg\,2\phi = 2V_{12}/(E_1-E_2),$$

and V_{12} is the interaction energy between two transition dipole moments. The functions Ψ_S and Ψ_A are stationary, but the conditions of femtosecond photoexcitation in PS I allow non-stationary function (Ψ) to be obtained as a superposition of Ψ_S and Ψ_A:

$$\begin{aligned}\Psi &= c_S\Psi_S + c_A\Psi_A \\ &= (c_S\cos\phi\exp\{-(i/\hbar)E_St\} - c_A\sin\phi\exp\{-(i/\hbar)E_At\})\psi_1 + \\ &\quad + (c_S\sin\phi\exp\{-(i/\hbar)E_St\} + c_A\cos\phi\exp\{-(i/\hbar)E_At\})\psi_2 = \\ &= c_1\psi_1 + c_2\psi_2.\end{aligned} \qquad (5)$$

It can be seen that $|c_1|^2$ and $|c_2|^2$ reflect the time dependence of the formation and the decay of the bleaching at 690 and 705 nm, respectively. Under conditions of femtosecond photoexcitation of PS I it was obtained at $t=0$ that $|c_1|^2 = 1$ and $|c_2|^2 = 0$; at $t>0$, $|c_1|^2 + |c_2|^2 = 1$. It can be shown that these expressions are valid at different ϕ, if $c_S = \cos\phi$ and $c_A = -\sin\phi$. Then:

$$|c_1|^2 = \cos^4(\phi) + \sin^4(\phi) + 0.5\sin^2(2\phi)\cos(\Delta Et/\hbar), \qquad (6)$$
$$|c_2|^2 = 0.5\sin^2(2\phi)(1 - \cos(\Delta Et/\hbar)),$$

where $\Delta E = E_S - E_A$. If $\phi = 45°$ and $\Delta Et/\hbar = \pi$, then $|c_1|^2 = 0$ and $|c_2|^2 = 1$, etc., i.e. excitation energy is transferred back and forth between chromophores with the period determined by ΔE (quantum beats) until some additional process blocks the coherent oscillations. In the case of PS I this block is evidently related to electron transfer between chromophores. The ratio $\Delta A_{705}/\Delta A_{690}$ measured and presented in Fig. 2C should correspond to the ratio $|c_2|^2/|c_1|^2$ presented in Fig. 2C as a solid line. The ΔE is equal to 247 cm^{-1} according to the difference between transition energies at 692 and 704 nm in equilibrium state (difference spectrum at 66 fs in Fig. 2A). For energy equal to 240 cm^{-1} the theoretical curve presented in Fig. 2C coincides with experimental points for $\phi = 21°$. In this case the ratio $2V_{12}/(E_1 - E_2)$ is close to 0.9.

At time intervals longer than 80 fs the theoretical curve decays to zero at $\Delta Et/\hbar = 2\pi$, while experimentally observed ratio $\Delta A_{705}/\Delta\alpha_{690}$ remains almost constant until ~10 ps (see Fig. 1). This shows that excited state distribution between A_0 and P700 is probably related to the electron density distribution (~50/50) between LUMO and HOMO orbitals of these chromophores accompanied by electron transfer leading to the formation of P700$^+$A$_0^-$ (Fig. 6). The formation of P700$^+$A$_0^-$ is a reason for the deviation between the theoretical curve of the quantum beat model and the observed ratio $\Delta A_{705}/\Delta\alpha_{690}$ in the time domain between 80 fs and 10 ps.

The loss of initial 660-nm band at 50 fs (Fig. 2A) seems to be determined by a new situation when excited states ψ_1 and ψ_2 do not exist any longer and new superposition should include the wave-functions of ground states of A_0 and P700 (ψ_{1G} (E_{1G}) and ψ_{2G} (E_{2G}), respectively), because the "intermediary" states of the excitation of
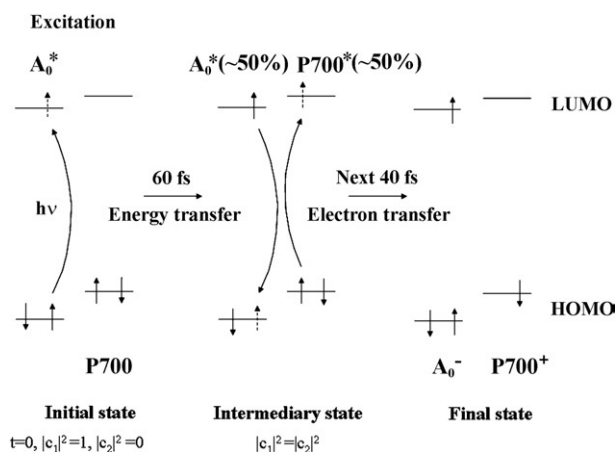

Fig. 6. Scheme of P700 and A_0 energy levels.

P700$^{\delta*}$ and $A_0^{\delta*}$ are formed. The appearance of a new superposition most probably is accompanied by femtosecond asymmetrical electron density shift from P700$^{\delta*}$ to $A_0^{\delta*}$ (like Wannier–Mott exciton formation) with a final formation of P700$^+$A$_0^-$ within 100 fs. At 60-fs delay the development of a new 660-nm band starts; it finishes within the next 40 fs. The developed band at 660 nm remains constant within a picosecond time range and then decays with time constant of ~26 ps in close relation to the electron transfer from A_0^- to A_1 with the formation of P700$^+$ spectrum with the maximum at 705 nm (Fig. 3B and D). In agreement with the reduction of *Chl* in solution [29], this result indicates that the band developed at 660 nm should belong to *Chl* anion radical (most probably A_0^-). Therefore, the development of a new 660-nm band directly confirms the formation of P700$^+$A$_0^-$ within the first 100 fs after the center of femtosecond excitation. In other words, due to the difference between redox potentials existing between LUMO and HOMO orbitals of P700 and A_0, the 50%-distribution of the excited states between P700 and A_0 achieved in ~60 fs cannot persist for a long time and is distorted with the formation of P700$^+$A$_0^-$ within the next 40 fs (Fig. 6).

The structure of the PS I RCs in which a *Chl* dimer P700 is revealed in optical measurements and in X-ray structure with the Mg-to-Mg distance of 6.3 Å and distance between *Chl* macrocycles of 3.6 Å was described [1]. This *Chl* arrangement in P700 is similar to that of P870 in bacterial RCs. However, in contrast to BRC and PS II, the primary acceptor of PS I RCs (A_0) is represented by a dimer of *Chl* molecules, though with smaller excitonic interaction than in P700 [37]. A relatively strong excitonic interaction between six *Chl* molecules (*A1*, *A2*, *A3*, *B1*, *B2*, and *B3*) and their dimers with femtosecond formation of the Frenkel and later the Wannier–Mott excitons might be the reason that among findings of intrinsic primary charge separation time for BRC (~3 ps at 293 K [38,39]) and PS II RC (~1 ps at 293 K [40]) the formation of the state P700$^+$A$_0^-$ demonstrates the maximal rate of the reaction with a time constant less than 100 fs.

5. Conclusions

The 20-femtosecond pump–probe experiments with low-energy laser pulses centered at 720 nm revealed very fast (<100 fs) conversion of delocalized exciton into charge-separated state between the primary donor P700 (bleaching at 705 nm) and the primary acceptor A_0 (bleaching at 690 nm) in PS I complexes isolated from *Synechocystis* sp. PCC 6803 cells. However another mechanism of charge separation under different excitation conditions cannot be ruled out.

The main spectral and kinetic features in favor of this conclusion can be summarized as follows:

i. The earliest absorbance changes (close to zero delay) with a bleaching at 690 nm are similar to the product of the absorption

spectrum of PS I complex and the laser pulse spectrum, which represents the efficiency spectrum of the light absorption by PS I upon femtosecond excitation centered at 720 nm;

ii. During the first ~60 fs energy transfer from the *Chl* species bleaching at 690 nm to the *Chl* bleaching at 705 nm occurs, resulting in almost equal bleaching of the two forms with the formation of delocalized exciton between 690-nm and 705-nm *Chl*s;

iii. Within the next ~40 fs the formation of a new broad band centered at ~660 nm (attributed to the appearance of *Chl* anion radical) is observed; this band decays with time constant of 26 ps simultaneously with an electron transfer to A_1;

iv. The subtraction of kinetic difference absorption spectra of the PS I RC closed state ($P700^+A_0A_1$) from that of the open state ($P700A_0A_1$) reveals the pure spectrum of the $P700^+A_0^-$ ion–radical pair.

A simple kinetic scheme taking into account the fast (<100 fs) charge separation was suggested to fit the experimental data in the time window of 60 fs–90 ps and in the spectral region of 410–730 nm: $An^* \xrightarrow{k1} [(PA_0)^*A_1] \xrightarrow{<100\,fs} P^+A_0^-A_1 \xrightarrow{k2} P^+A_0A_1^-$. The global fitting procedure based on singular value decomposition analysis revealed the ~5-ps energy transfer from antenna *Chl** to $P700A_0A_1$ in the remaining part of the RCs and ~25-ps formation of the secondary radical pair $P700^+A_0A_1^-$.

Acknowledgements

Appendix A. Supplementary data

Supplementary data associated with this article can be found, in the online version, at doi:10.1016/j.bbabio.2010.02.026.

References

[1] P. Jordan, P. Fromme, H.T. Witt, O. Klukas, W. Saenger, N. Krauß, Three-dimensional structure of cyanobacterial photosystem I at 2.5 Å resolution, Nature 411 (2001) 909–917.

[2] V.V. Ptushenko, D.A. Cherepanov, L.I. Krishtalik, A.Yu. Semenov, Semi-continuum electrostatic calculations of redox potentials in photosystem I, Photosynth. Res. 97 (2008) 55–74.

[3] J. Deisenhofer, O. Epp, K. Miki, R. Huber, H. Michel, Structure of the protein subunits in the photosynthetic reaction center of *Rhodopseudomonas viridis* at 3 Å resolution, Nature 318 (1985) 618–624.

[4] J.P. Allen, G. Feher, T.O. Yeates, H. Komiya, D.C. Rees, Structure of the reaction center from *Rhodobacter sphaeroides* R-26: The cofactors, Proc. Natl. Acad. Sci. U. S. A. 84 (1987) 5730–5734.

[5] M. Guergova-Kuras, B. Boudreaux, A. Joliot, P. Joliot, K. Redding, Evidence for two active branches for electron transfer in photosystem I, Proc. Natl. Acad. Sci. U. S. A. 98 (2001) 4437–4442.

[6] W. Xu, P.R. Chitnis, A. Valieva, Art van der Est, K. Brettel, M. Guergova-Kuras, Y.N. Pushkar, S.G. Zech, D. Stehlik, G. Shen, B. Zybailov, J.H. Golbeck, Electron transfer in cyanobacterial photosystem I: II. Determination of forward electron transfer rates of site-directed mutants in a putative electron transfer pathway from A_0 through A_1 to F_X, J. Biol. Chem. 278 (2003) 27876–27887.

[7] K. Brettel, W. Leibl, Electron transfer in photosystem I, Biochim. Biophys. Acta 1507 (2001) 100–114.

[8] N.V. Karapetyan, E. Schlodder, R. van Grondelle, P. Dekker, Photosystem I, in: J. Golbeck (Ed.), The Light-Driven Plastocyanin:Ferredoxin Oxidoreductase, Springer, Dordrecht, 2006, pp. 177–192.

[9] G. Hastings, F.A.M. Kleinherenbrink, S. Lin, T.J. McHugh, R.E. Blankenship, Observation of the reduction and reoxidation of the primary electron acceptor in photosystem I, Biochemistry 33 (1994) 3193–3200.

[10] S. Savikhin, W. Xu, P. Martinsson, P.R. Chitnis, W.S. Struve, Kinetics of charge separation and $A_0 \rightarrow A_1$ electron transfer in photosystem I reaction centers, Biochemistry 40 (2001) 9282–9290.

[11] S. Savikhin, Photosystem I, in: J. Golbeck (Ed.), The Light-Driven Plastocyanin: Ferredoxin Oxidoreductase, Springer, Dordrecht, 2006, pp. 155–175.

[12] S. Kumazaki, I. Ikegami, H. Furusawa, S. Yasuda, K. Yoshihara, Observation of the excited state of the primary electron donor chlorophyll (P700) and the ultrafast charge separation in the spinach photosystem I reaction center, J. Phys. Chem. B 105 (2001) 1093–1099.

[13] V.A. Shuvalov, A.M. Nuijs, H.J. van Gorkom, H.W.J. Smit, L.N.M. Duysens, Picosecond absorbance changes upon selective excitation of the primary electron donor P700 in photosystem I, Biochim. Biophys. Acta 850 (1986) 319–323.

[14] A.M. Nuijs, V.A. Shuvalov, H.J. van Gorkom, J.J. Plijter, L.N.M. Duysens, Picosecond absorbance difference spectroscopy on the primary reactions and the antenna-excited states in photosystem I particles, Biochim. Biophys. Acta 850 (1986) 310–318.

[15] S. Savikhin, W. Xu, P.R. Chitnis, W.S. Struve, Ultrafast primary processes in PS I from *Synechocystis* sp. PCC 6803: roles of P700 and A_0, Biophys. J. 79 (2000) 1573–1586.

[16] N.T.H. White, G.S. Beddard, J.R.G. Thorne, T.M. Feehan, T.E. Keyes, P. Heathcote, Primary charge separation and energy transfer in the photosystem I reaction center of higher plants, J. Phys. Chem. 100 (1996) 12086–12099.

[17] A.N. Melkozernov, S. Lin, R.E. Blankenship, Excitation dynamics and heterogeneity of energy equilibration in the core antenna of Photosystem I from the cyanobacterium *Synechocystis* sp. PCC 6803, Biochemistry 39 (2000) 1489–1498.

[18] B. Gobets, R. van Grondelle, Energy transfer and trapping in photosystem I, Biochim. Biophys. Acta 1507 (2001) 80–99.

[19] M.G. Muller, J. Niklas, W. Lubitz, A.R. Holzwarth, Ultrafast transient absorption studies on photosystem I reaction centers from *Chlamydomonas reinhardtii*. 1. A new interpretation of the energy trapping and early electron transfer steps in photosystem I, Biophys. J. 85 (2003) 3899–3922.

[20] K. Gibasiewich, V.M. Ramesh, A.N. Melkozernov, S. Lin, N.W. Woodbury, R.E. Blankenship, A.N. Webber, Excitation dynamics in the core antenna of PS I from *Chlamydomonas reinhardtii* CC 2696 at room temperature, J. Chem. 105 (2001) 11498–11506.

[21] K. Gibasiewich, V.M. Ramesh, S. Lin, K. Redding, N.W. Woodbury, A.N. Webber, Excitonic interactions in wild-type and mutant PS I reaction centers, Biophys. J. 85 (2003) 2547–2559.

[22] A.R. Holzwarth, M.G. Muller, J. Niklas, W. Lubitz, Ultrafast transient absorption studies on photosystem I reaction centers from *Chlamydomonas reinhardtii*. 2. Mutations near the P700 reaction center chlorophylls provide new insight into the nature of the primary electron donor, Biophys. J. 90 (2006) 552–565.

[23] G. Shen, J. Zhao, S.K. Reimer, M.L. Antonkine, Q. Cai, S.M. Weiland, J.H. Golbeck, D.A. Bryant, Assembly of Photosystem I, J. Biol. Chem. 277 (2002) 20343–20354.

[24] E.N. Ushakov, V.A. Nadtochenko, S.P. Gromov, A.I. Vedernikov, N.A. Lobova, M.V. Alfimov, F.E. Gostev, A.N. Petrukhin, O.M. Sarkisov, Ultrafast excited state dynamics of the bi- and termolecular stilbene–viologen charge-transfer complexes assembled via host-guest interactions, Chem. Phys. 298 (2004) 251–261.

[25] A.L. Dobryakov, J.L. Pérez Lustres, S.A. Kovalenko, N.P. Ernsting, Femtosecond transient absorption with chirped pump and supercontinuum probe: perturbative calculation of transient spectra with general lineshape functions, and simplifications, Chem. Phys. 347 (2008) 127–138.

[26] D. Mi, S. Lin, R.E. Blankenship, Picosecond transient absorption spectroscopy in the blue spectral region of photosystem I, Biochemistry 38 (1999) 15231–15237.

[27] V.A. Shuvalov, A.G. Yakovlev, L.G. Vasilieva, A.Ya. Shkuropatov, Photosystem I, in: J. Golbeck (Ed.), The Light-Driven Plastocyanin:Ferredoxin Oxidoreductase, Springer, Dordrecht, 2006, pp. 291–300.

[28] B. Ke, The rise time of photoreduction difference spectrum and oxidation–reduction potential of P430, Arch. Biochem. Biophys. 152 (1972) 70–77.

[29] I. Fujita, M.S. Davis, J. Fajer, Anion radicals of pheophytin and chlorophyll a: their role in the primary charge separations of plant photosynthesis, J. Am. Chem. Soc. 100 (1978) 6280–6282.

[30] R. Croce, D. Dorra, A.R. Holzwarth, R.C. Jennings, Fluorescence decay and spectral evolution in intact Photosystem I of higher plants, Biochemistry 39 (2000) 6341–6348.

[31] P. Mathis, I. Ikegami, P. Setif, Nanosecond flash-studies of the absorption spectrum of the photosystem I primary acceptor A_0, Photosynth. Res. 16 (1988) 203–210.

[32] W. Giera, S. Lin, A. Webber, K. Gibasiewicz, V.M. Ramesh, Electron transfer from A to A(1) in Photosystem I from *Chlamydomonas reinhardtii* occurs in both the A and B branch with 25–30-ps lifetime, Phys. Chem. Chem. Phys. 11 (2009) 5186–5191.

[33] N.P. Ernsting, S.A. Kovalenko, T. Senyushkina, J. Saam, V. Farztdinov, Wave-packet-assisted decomposition of femtosecond transient ultraviolet–visible absorption spectra: application to excited-state intramolecular proton transfer in solution, J. Phys. Chem. A 105 (2001) 3443–3453.

[34] F.A.M. Kleinherenbrink, G. Hastings, B.P. Wittmershaus, R.E. Blankenship, Delayed fluorescence from Fe–S type photosynthetic reaction centers at low redox potential, Biochemistry 33 (1994) 3096–3105.

[35] G.D. Macomber, The Dynamics of Spectroscopic Transition, John Wiley and Sons, New York–London–Sydney–Toronto, 1976.

[36] V.A. Shuvalov, Main features of the primary charge separation in photosynthetic reaction centers, in: C. Sybesma (Ed.), Nijhoff Martinus, Dr.W. Junk Publishers,

Advances in Photosynthesis Research, The Hague/Boston/Lancaster, 1984, pp. 93–100.

[37] T. Renger, E. Schlodder, Modeling of optical spectra and light harvesting in photosystem I, in: J. Golbeck (Ed.), The Light-Driven Plastocyanin: Ferredoxin Oxidoreductase, Springer, Dordrecht, 2006, pp. 595–610.

[38] A.G. Yakovlev, V.A. Shuvalov, A. Ya. Shkuropatov, Nuclear wave packet motion between P* and $P^+B_A^-$ potential surfaces with a subsequent electron transfer to HA in bacterial reaction centers at 90 K, Biochemistry 41 (2002) 14019–14027.

[39] A.G. Yakovlev, T.A. Shkuropatova, L.G. Vasilieva, P. Gast, A. Ya. Shkuropatov, V.A. Shuvalov, Vibrational coherence in bacterial reaction centers with genetically modified B-branch pigment composition, Biochim. Biophys. Acta 1757 (2006) 369–379.

[40] I.V. Shelaev, F.E. Gostev, V.A. Nadtochenko, A.Ya. Shkuropatov, A.A. Zabelin, M.D. Mamedov, A.Yu. Semenov, O.M. Sarkisov, V.A. Shuvalov, Primary light-energy conversion of photosystem II and bacterial reaction centers: II. Femto- and picosecond charge separation in PS II D1/D2/Cytb559 complex, Photosynth. Res. 98 (2008) 95–103.